Adsorption of Hg^{2+} on a Novel Chelating Fiber Prepared by Preirradiation Grafting and Amination

Ying Yang,[1] Nianfang Ma,[1] Qikun Zhang,[1] Shuixia Chen[1,2]

[1]*Polymeric Composite and Function Materials (PCFM) Laboratory, Optoelectronic and Functional Composite Materials (OFCM) Institute, School of Chemistry and Chemical Engineering, Sun Yat-Sen University, Guangzhou 510275, People's Republic of China*
[2]*Materials Science Institute, Sun Yat-Sen University, Guangzhou 510275, People's Republic of China*

Received 20 November 2008; accepted 2 March 2009
DOI 10.1002/app.30355
Published online 8 May 2009 in Wiley InterScience (www.interscience.wiley.com).

ABSTRACT: A novel chelating fiber was prepared by the irradiation-induced grafting copolymerization of glycidyl methacrylate on polypropylene fiber and consequent amination with diethylenetriamine. The effects of the reaction conditions, such as reaction time, temperature, and monomer concentration, on the degree of grafting were investigated. The optimal conditions for grafting were found to be 3 h, 100°C, and a 50% (v/v) glycidyl methacrylate concentration in tetrahydrofuran solution. This fiber showed good adsorption performance at different concentrations of Hg^{2+}, in particular for trace Hg^{2+}. Under the adsorption conditions of pH = 4, initial concentration = 1000 mg/L, and time = 20 h, the adsorption capacity of the chelating fiber for Hg^{2+} reached 785.28 mg/g. It completely adsorbed the Hg^{2+} ions in solution within a short contact time, showing a very high adsorption rate for Hg^{2+}. Furthermore, the chelating fiber also had a high selectivity for mercury, whereas Cu^{2+} coexisted in different concentrations. © 2009 Wiley Periodicals, Inc. J Appl Polym Sci 113: 3638–3645, 2009

Key words: adsorption; fibers; graft copolymers; ion exchangers

INTRODUCTION

Mercury, which is widely used and extremely toxic at relatively low dosages, is one of the principle heavy metals responsible for causing fetal injuries and eventually death, as it can pass easily through the blood–brain barrier and affect the fetal brain.[1–4] The safe limits for inorganic mercury in drinking water and industrial wastewater[5] are 1.0 and 5 μg/L, respectively. Therefore, mercury remediation has become a critical global need. A number of methods have been explored for the remediation of mercury pollution.[6–15] The adsorption process is one effective technique that has been successfully used for metal removal from wastewater. A wide range of adsorbents, including fly ash, coal, tree bark, human hair, fertilizer waste, activated carbon fiber, and ion-exchange resins, have been used to remove mercury from wastewaters. As an effective method, chelating fibers and resins[16–19] are very important adsorbents for metal-ion complexation because of their hydrophilicity, accessibility, and high capacity. Fibrous chelate materials have several advantages over conventional chelate beads.[20] For example, they are easier to prepare and display greatly improved contact efficiencies with metal ions. The adsorption efficiency for heavy-metal ions by chelating fibers are usually affected by the surface functional groups of the adsorbents. Amino groups are well-established chelating groups[21] that have been found to be one of the most effective chelating functional groups for the adsorption or removal of heavy-metal ions from aqueous solutions.

The graft polymerization of glycidyl methacrylate (GMA) onto polymer substrates is advantageous for the further modification of grafted products because the epoxy group of GMA reacts easily with other groups. Choi and coworkers,[22,23] Grasselli et al.,[24] and Konishi et al.[25] introduced iminodiacetate and other amino chelating groups onto the polyethylene membrane for the purpose of removing heavy-metal ions such as Co^{2+}, Cs^{1+}, Pd^{2+}, and Pb^{2+} from aqueous solutions.

In this study, a novel chelating fiber with amino groups was prepared by the radiation-induced grafting of GMA onto polypropylene (PP) fiber and consequent amination with diethylenetriamine (DETA). The effects of the reaction conditions on the grafting degree were studied. The adsorption properties of the fiber for Hg^{2+} were evaluated.

EXPERIMENTAL

Chemicals

PP fiber was kindly provided by Lanzhou Refinery (China). GMA and DETA were purchased from

Correspondence to: S. Chen (cescsx@mail.sysu.edu.cn).

Sigma–Aldrich Co. (Shanghai, China) The analytical-grade reagents acetone, tetrahydrofuran (THF), hydrochloric acid (HCl), sulfuric acid (H_2SO_4), nitric acid (HNO_3), mercuric chloride ($HgCl_2$), stannous chloride ($SnCl_2$), and cupric chloride ($CuCl_2$) were used without further purification. The guaranteed-grade reagents H_2SO_4 and HNO_3 were used for the quantitative analysis of mercury. Deionized water was used to prepare all solutions in the study.

GMA grafting on PP fiber

PP fibers cleaned with acetone were sealed in a polyethylene bag and subjected to γ-ray irradiation in the presence and absence of air for a desired time. After irradiation, the preirradiated PP fibers with enough dryer were sealed and placed in a refrigerator at 4°C for future use. Certain amounts of GMA, THF, and preirradiated PP fibers were added to a 100-mL, three-necked flask and then bubbled with nitrogen during reaction to keep the reactant from oxygen. The grafting reaction was carried out at a fixed temperature for a certain time. After the reaction, the grafted fibers were taken out and extracted in a Soxhlet apparatus with THF to remove the residual monomer and homopolymer. The grafted PP (PP-*g*-GMA) fibers were dried in a vacuum oven at 60°C and then weighed. The grafting degree (*G*) was obtained by the following formula:

$$G\ (\%) = \frac{W_g - W_0}{W_0} \times 100\% \quad (1)$$

where W_0 and W_g are the weights of the original and grafted PP fibers, respectively.

Amination reaction

The grafted PP-*g*-GMA fibers, 50 mL of DETA, and 5 g of $AlCl_3 \cdot 6H_2O$ were added to a 100-mL flask, and the mixture was suspended by a stirrer. Excess DETA was used for the solvent and reactant. The reaction was carried out at 120°C for 3 h with stirring. After the reaction, the aminated chelating fiber (ACHF) was isolated and washed with deionized water and acetone in order and then dried at 60°C *in vacuo*.

Figure 1 shows the preparation procedure of the radiation grafting of GMA onto PP and the introduction of the amino groups.

Characterization methods

IR spectra were obtained with a Fourier transform infrared (FTIR) analyzer (Nicolet/Nexus 670, USA). FTIR/attenuated total reflection measurements were carried out in the range 4000–650 cm^{-1}, with a continuum microscope and attenuated total reflection objective.

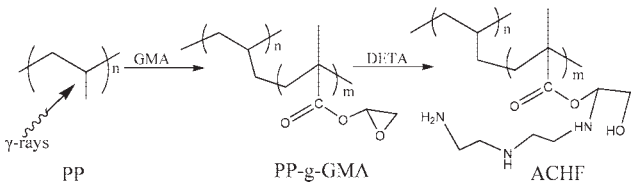

Figure 1 Preparation of the chelating fiber ACHF.

A Netzsch TG-209 (Selb, Germany) thermogravimetry analyzer was used for thermal stability determination of all of the samples. The thermograms were obtained under a nitrogen atmosphere at a procedure heating rate of 10°C/min from ambient temperature to 600°C.

The mechanical properties of the fibers were characterized by a Monofilament Mightiness instrument (YG001A Textile Mill, Taicang, China). All tensile testing was performed with an analog controller equipped with a 100-kN load cell. Breaking load was measured in terms of the breaking force in centi-Newtons. Ten parallel stochastic filaments of each sample were tested with 10 mm of gauge length and at a 10 mm/min stretching speed. Then, the average value was calculated.

Thermal field emission environmental scanning electron microscopy (SEM; Quanta 400F, Fei, The Netherlands) and energy dispersive X-ray spectroscopy (Inca, Oxford, United Kingdom) were used to characterize the surface morphology of ACHF.

Adsorption and analytical procedures

So that we could ignore the degree of grafting and aminating rate, the fibers used in all of the adsorption experiments were from the same batch of samples. The effect of pH value on the adsorption was studied at pH values of 1.0, 2.0, 3.0, 4.0, 5.0, 6.0, and 7.0. The pH value of the solutions was adjusted with HNO_3. Dried samples of ACHF (ca. 0.1 g) were added to a 100-mL Erlenmeyer flask containing 100 mL of the Hg^{2+} ion solution (100 mg/L) and adjusted to the desired pH. Then, the flasks were sealed and shaken for 24 h at 30°C. The effect of the initial concentration of Hg^{2+} on the adsorption capacity was studied in the range 0–1000 mg/L. The effect of the adsorption time on the adsorption capacity was investigated in the range 0–600 min when the initial concentrations of Hg^{2+} were 123 mg/L and 500 μg/L. The dynamic adsorption curves were investigated in the range 0–3000 mL of influent volume when the initial concentrations of Hg^{2+} were 55 mg/L and 100 μg/L. At this time, about 0.5 g of fiber was cut into pieces and immersed in distilled water for 0.5 h and then put into an adsorption column with a radius equal to 0.5 cm. The length of

the column bed was about 5 cm. The flow rate of the influent solution through the fiber was 2 mL/min and was controlled by a peristaltic pump (MasterFlex, Cole-Parmer Instrument Co., USA). The effect of the coexistent Cu^{2+} ion on the adsorption for Hg^{2+} was investigated in the concentration range 0–1000 mg/L when the initial concentration of Hg^{2+} was 100 mg/L.

The residual concentration of Hg^{2+} in the solution was determined by cold atomic absorption spectrometry with a model F732-V Intelligent mercury analyzer (Shanghai Huaguang Instrument Co., Shanghai, China). The concentration of Cu^{2+} in the solution was determined with a Hitachi (Tokyo, Japan) Z-2000 flame atomic absorption spectrometer.

The adsorption amount [Q (mg/g)] was calculated as follows:

$$Q = V(C_0 - C_e)/W \quad (2)$$

where W is the weight of ACHF (g), V is the volume of the solution (L), and C_0 and C_e are the concentrations (mg/L) of Hg^{2+} or Cu^{2+} before and after adsorption, respectively.

RESULTS AND DISCUSSION

Effects of the reaction conditions on the grafting degree of PP-*g*-GMA

Figure 2 shows the effects of the reaction temperature and reaction time on the grafting degree of the PP fibers. The results indicate that the grafting degree reached its highest value, 102 wt %, at 100°C with a reaction time of 3 h. As is well known, a higher temperature facilitates the diffusion of GMA monomers to the active sites of the PP fibers and speeds up the process of peroxide decomposition to form radical groups, which thus leads to a higher grafting degree. However, a high temperature also rapidly accelerates the decay of alkyl radicals and the homopolymerization of GMA monomers. The dual-termination reaction accelerated at a higher temperature of radicals has an adverse impact on the graft reaction. In addition, from the thermodynamic point of view, the grafting reaction is a exothermic process. It will be negative for the reaction when the temperature is too high. The optimal reaction temperature is 100°C.

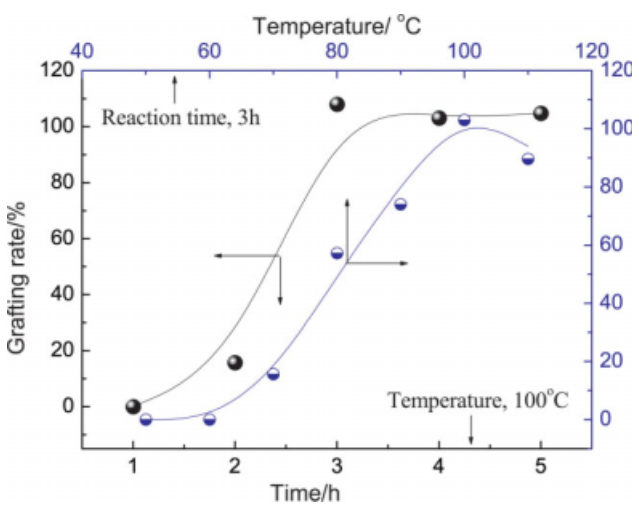

Figure 2 Effects of the reaction temperature and reaction time on the grafting degree (PP, 0.5 g; GMA monomer concentration, 35%). [Color figure can be viewed in the online issue, which is available at www.interscience.wiley.com.]

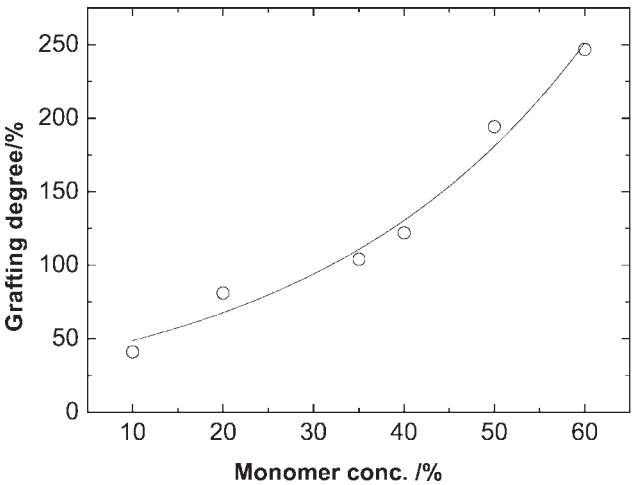

Figure 3 Effect of the concentration of the monomer on the grafting degree (PP, 0.5 g; reaction time, 3 h; temperature, 100°C).

As it took a certain amount of time for the fiber to be completely swollen to react with the graft monomer, the grafting degree was slower at the initial stage. However, the grafting degree rapidly increased from 20% to about 100% with the reaction time increasing from 2 to 3 h (Fig. 3); this indicated that, in addition to that caused by free radicals, the grafting reaction was also triggered by the decomposition of the macromolecular peroxides in the fiber that formed by oxidation with air. After 3 h of reaction, the grafting degree did not obviously increase any more, which indicated that the grafting reaction approached equilibrium because of the decreases in the GMA monomer concentration and in the number of peroxides and free radicals.

The effect of the concentration of monomer on the grafting degree is shown in Figure 3. Increasing monomer concentration increased the grafting degree of PP fibers; however, it also resulted in the formation of a large amount of homopolymers. When the monomer concentration was too high, the GMA monomers had more of a chance to form

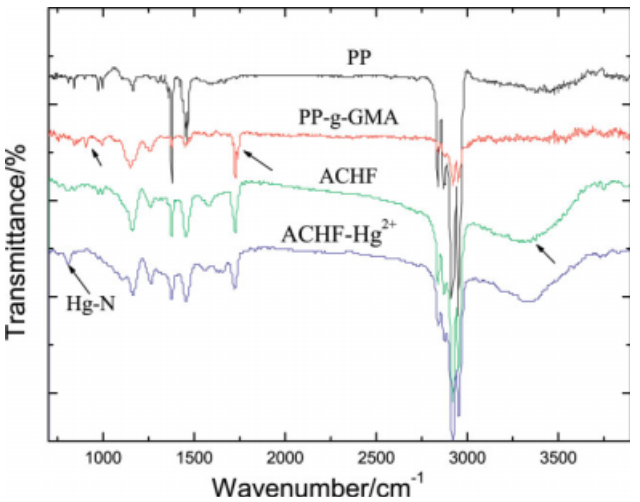

Figure 4 FTIR spectra of the original PP fiber, PP-*g*-GMA, ACHF, and Hg^{2+}-chelated ACHF. [Color figure can be viewed in the online issue, which is available at www.interscience.wiley.com.]

homopolymers, which increased the viscosity of the system; this impeded the grafting reaction and resulted in a lower grafting degree.

Chemical structure of the fibers

Figure 4 shows the IR spectra of PP, PP-*g*-GMA, ACHF, and Hg^{2+}-chelated ACHF. Compared with the spectrum of the PP fiber, the spectrum of the PP-*g*-GMA changed obviously; new absorption peaks of 1730 (—C=O stretching), 1150 and 1380 (C—O—C), and 908 cm^{-1} (epoxy ring stretching) were observed in PP-*g*-GMA, which confirmed that GMA was grafted on the PP fiber. The spectrum of the ACHF showed stronger and wider absorption bands at 3200–3400 cm^{-1}, which belonged to N—H bonds in the —NH— and $—NH_2$ groups, and the bands at 1570 and 1660 cm^{-1} were attributed to the stretching vibrations of N—H bonds. In addition, the absorption peak of 908 cm^{-1} disappeared. These results indicate that the epoxy groups of GMA were modified with DETA. In the FTIR spectra of Hg^{2+}-chelated ACHF, we found that the absorption bands of N—H at 3200–3400 cm^{-1} became weak, and a new peak at 820 cm^{-1} for N—Hg arose; this provided evidence of the chelation of mercury ions by ACHF.

Tensile strength of the fibers

Table I shows the elongation and tensile strength of the PP fiber and ACHF. There were increases in both the elongation and tensile strength of ACHF. After GMA grafting and consequent amination modification, the fibers contained $—NH_2$, —NH—, and —OH groups, and they easily formed hydrogen bonds when they were close to each other. FTIR showed strong and broad bands at 3200–3400 cm^{-1}, which proved that the N—H bonds included hydrogen bonds and nonhydrogen bonds. Thus, ACHF showed better elasticity and flexibility than the original PP because of the formation of hydrogen bonds, which increased the interactions of molecules.

TABLE I
Mechanical Properties of PP and ACHF Fibers

Fiber	Elongation (mm)	Tensile strength (cN)
PP	2.3	11.5
ACHF	2.8	16.9
Increment (%)	47	22

Thermal stability of the fibers

The thermogravimetric analysis results of the PP fiber, PP-*g*-GMA, and ACHF are presented in Figure 5. The PP fiber showed only one platform at a mass loss of around 100%; this was because the PP fiber was converted into CO_2 and H_2O completely at the decomposition temperature. For PP-*g*-GMA, two platforms appeared, and the starting decomposition temperatures were at 338 and 448°C, respectively. We believe that the first platform came from the easy degradation nature of the grafted GMA molecules. With respect to ACHF, it had a lower thermal stability than PP-*g*-GMA. Three platforms appeared: the initial loss at about 150–200°C was the grafted molecule DETA, and the second platform came from the easy degradation nature of the grafted molecules GMA. The decomposition temperature of ACHF declined, but it could still meet requirements for use.

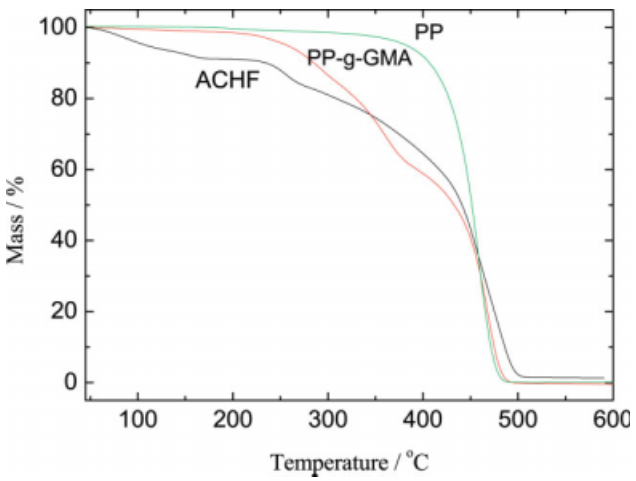

Figure 5 Thermogravimetric analysis results for the PP fiber, PP-*g*-GMA, and ACHF. [Color figure can be viewed in the online issue, which is available at www.interscience.wiley.com.]

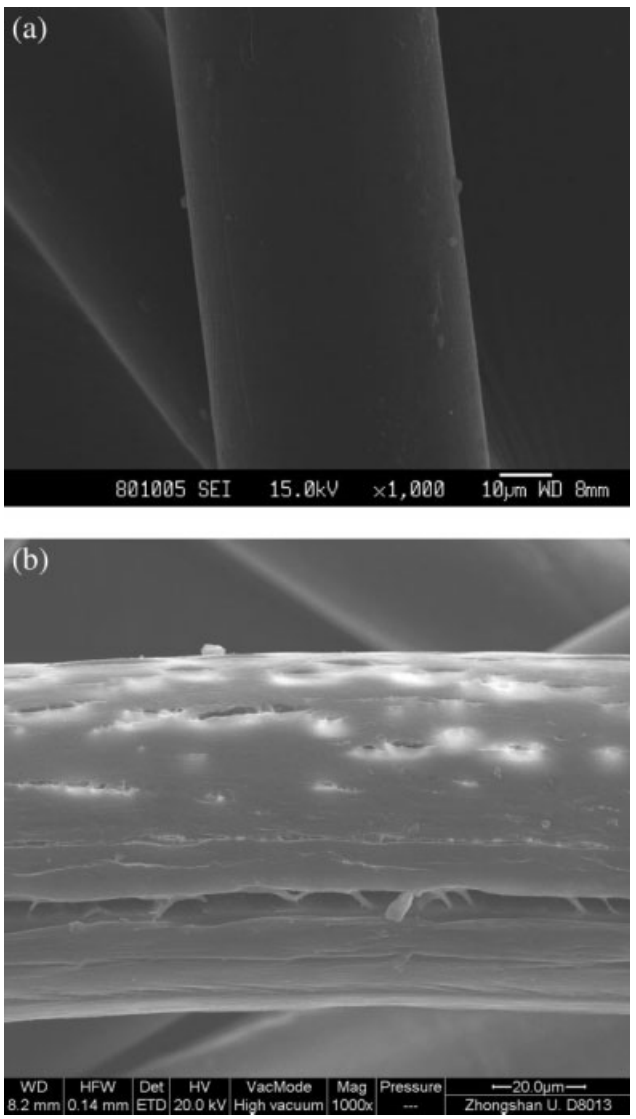

Figure 6 SEM photographs of (a) the original PP and (b) ACHF.

SEM photographs

As observed with the naked eye, the states of the fiber before and after reaction showed no other obvious changes in addition to the change in color from white to yellow. Figure 6 shows the SEM photographs of the original PP and ACHF; the surfaces of the PP fiber became rough and showed a lot of cracks after preirradiation grafting and amination.

Batch adsorption behavior of ACHF for Hg^{2+}

Effect of pH on adsorption

Considering the different forms of Hg^{2+} that would exist at different pH values, we studied pH values from 1.0 to 7.0, and the results are shown in Figure 7. When the pH was below 3, the adsorption capacity of ACHF for Hg^{2+} was lower. The adsorption capacity for Hg^{2+} ions increased gradually when the pH increased from 3 to 7 and reached a maximum 127.43 mg/g at pH = 6. The surface structure of the fiber and Hg^{2+} existed in different forms because of the different protonation and deprotonation behaviors of acidic and basic groups. At low pH values, the concentration of H^+ was much higher at the surface, and hydrogen bonds were formed among the amino groups, hydroxyls, and H^+. The large amount of H^+ also repelled the Hg^{2+} charged positively as a result of the electrostatic potential and prevented the Hg^{2+} adsorbed onto the surface of the fiber so that the adsorption capacity was lower. With increasing pH, the concentration of H^+ decreased, and the electrostatic repulsion decreased sharply, achieving a higher adsorption quantity. Therefore, the adsorption capacity for Hg^{2+} achieved optimal results with the adjustment of the pH value.

Effect of the initial concentration of Hg^{2+} on adsorption

The equilibrium adsorption capacity of ACHF for Hg^{2+} was investigated over a range of concentrations. The results are shown in Figure 8. They reveal that the adsorption capacity of Hg^{2+} increased almost linear with increasing initial concentration of Hg^{2+}. The adsorption capacity of ACHF for Hg^{2+} was up to 785.28 mg/g when the initial concentration was 1000 mg/L.

The experimental equilibrium adsorption data were fitted by both the Langmuir [eq. (3)] and Freundlich [eq. (4)] equations:

$$\frac{C_e}{Q_e} = \frac{1}{Q_m k_L} + \frac{C_e}{Q_m} \tag{3}$$

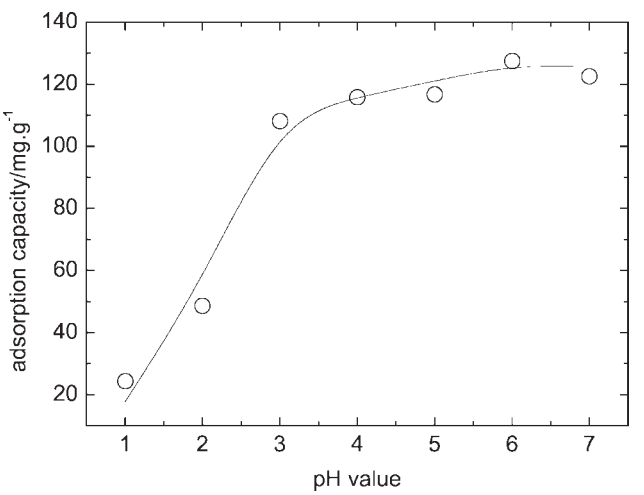

Figure 7 Effect of the pH value on the adsorption capacity of Hg^{2+} (C_0 = 100 mg/L, time = 24 h, temperature = 29.9°C).

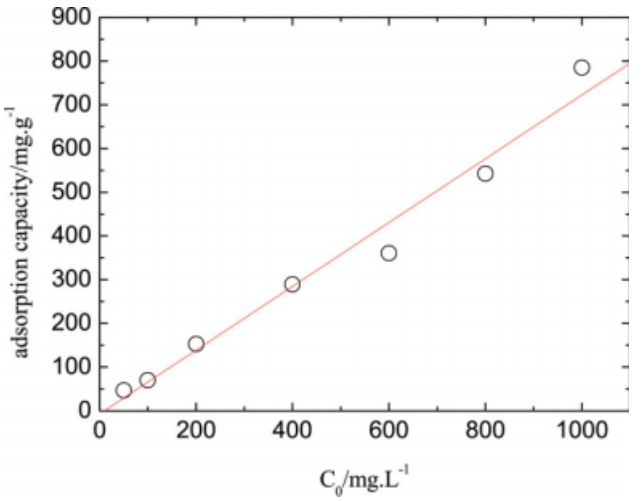

Figure 8 Adsorption capacity of ACHF for a high concentration of Hg^{2+} in water (pH = 4, time = 20 h, temperature = 29.9°C). [Color figure can be viewed in the online issue, which is available at www.interscience.wiley.com.]

$$\lg Q_e = \lg k_F + \frac{1}{n_F}\lg C_e \tag{4}$$

where Q_e and Q_m are the adsorption capacity at equilibrium and the maximum adsorption capacity (mg/g), respectively; C_e is the Hg^{2+} concentration (mg/L) in the solution at equilibrium; and k_L, k_F, and n_F are the adsorption equilibrium constants.

The corresponding fitting parameters and the correlation coefficients are presented in Table II. The Freundlich equation was found to best fit the adsorption isotherms. From the Langmuir equation, the maximum adsorption capacity of the ACHF for Hg^{2+} was calculated to be 1000 mg/g. Table III shows the comparison of the adsorption capacities of ACHF and other similar adsorbents. As shown in Table III, the adsorption capacity of ACHF prepared in this study was much higher than those of other successful Hg^{2+} adsorbents reported in the literature.

Adsorption rate for Hg^{2+}

The adsorption of ACHF for Hg^{2+} satisfied the absorption rate; especially in the initial adsorption process, the adsorption capacity increased with time until the residual concentration of Hg^{2+} reached zero. When the initial concentration of Hg^{2+} was 123 mg/L, the residual concentration of Hg^{2+} was 71.2 mg/L after adsorption for 30 min. The adsorption approached its equilibrium in about 120 min, and the residual concentration of Hg^{2+} approached zero, as shown in Figure 9. For the ppb level of Hg^{2+} adsorption, the initial concentration of Hg^{2+} was 500 μg/L, the residual concentration of Hg^{2+} reached 126.5 μg/L after adsorption for 10 min, the adsorption approached its equilibrium in about 60 min, and no Hg^{2+} in the residual solution was detected, as shown in Figure 10.

The kinetic data were fitted by a pseudo-first-order adsorption kinetic equation [eq. (5)] and a pseudo-second-order adsorption kinetic equation [eq. (6)]:

$$Q_t = Q_e(1 - e^{-k_1 t}) \tag{5}$$

$$\frac{t}{Q_t} = \frac{1}{k_2 Q_e^2} + \frac{t}{Q_e} \tag{6}$$

where t is the adsorption time; k_1 and k_2 are the pseudo-first-order adsorption rate constant and pseudo-second-order adsorption rate constant, respectively; and Q_t is the adsorption capacity at

TABLE II
Langmuir and Freundlich Isotherm Fitting Parameters

Langmuir model			Freundlich model		
Q_m (mg/g)	k_L (L/mg)	R	lg k_F	n_F	R
1000	0.004	0.542	1.136	1.592	0.953

TABLE III
Comparison of the Adsorption Capacities of Similar Adsorbents

Adsorbent	Adsorption capacity (mg/g)	Reference
ACHF	785.2	This work
Mesoporous silica	505	10
SBA-15 (molecular sieve)	220	13
MCM-41 (molecular sieve)	140	13
Natural zeolites	121	9
Sago carbon	55.6	12
PMPS fibers (chelating fiber)	32	15

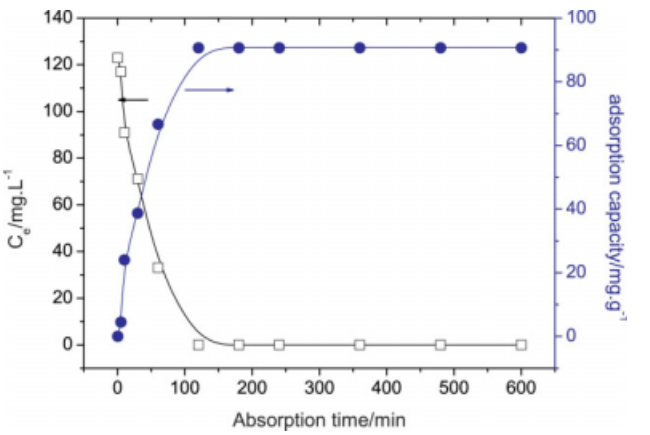

Figure 9 Adsorption curve for Hg^{2+} (pH = 4, C_0= 123 mg/L, and temperature = 30°C). [Color figure can be viewed in the online issue, which is available at www.interscience.wiley.com.]

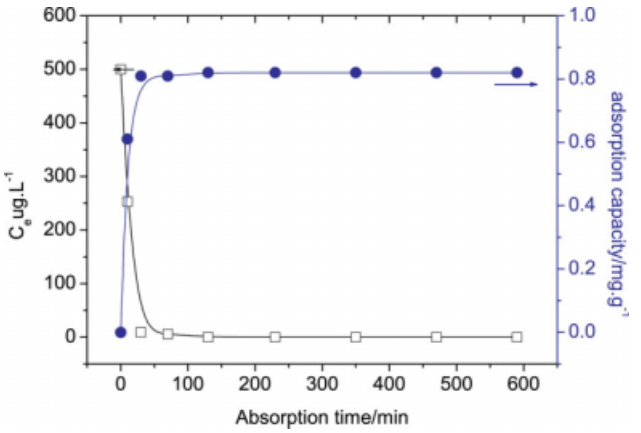

Figure 10 Adsorption curve for Hg^{2+} (pH = 4, C_0= 500 μg/L, and temperature = 30°C). [Color figure can be viewed in the online issue, which is available at www.interscience.wiley.com.]

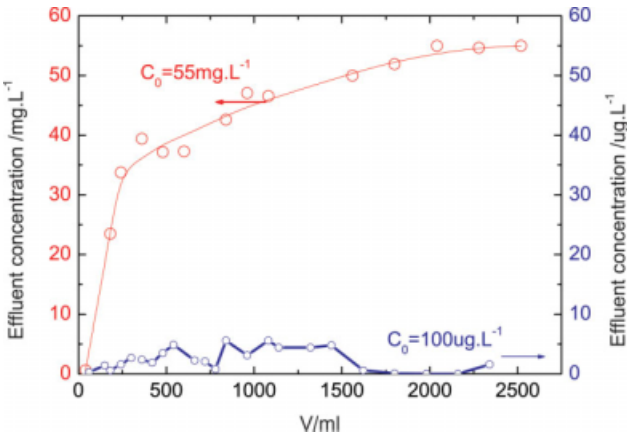

Figure 11 Dynamic adsorption curve for $Hg^{2+}$of ACHF (pH = 7, C_0= 55 mg/L or 100 μg/L, feed flow rate = 2 mL/min). [Color figure can be viewed in the online issue, which is available at www.interscience.wiley.com.]

time *t*. The results of the adsorption kinetics shown in Table IV indicate that the adsorption rates of ACHF for Hg^{2+} were very rapid. The adsorption processes of ACHF obeyed pseudo-second-order adsorption kinetics.

Dynamic adsorption

Figure 11 shows the dynamic adsorption behavior of Hg^{2+} on ACHF. It turned out that the adsorption for Hg^{2+} reached saturation over 2000 mL of influent volume when the feed concentration of Hg^{2+} was 55 mg/L. When the initial concentration of Hg^{2+} was 100 μg/L, the effluent concentration of Hg^{2+} ions was maintained lower than 5 μg/L throughout the experiment. This indicates that the fiber could be applied to remove the trace Hg^{2+} in wastewater to meet the standards of discharge for industrial wastewater. The fiber has great practical potential to treat mercury-containing wastewater, particularly for trace Hg^{2+}.

Effect of the coexistence of Cu^{2+} ions on the adsorption of Hg^{2+}

In our previous studies, we found that cheating fibers with amino groups had high adsorption capacities for Cu^{2+}, so the effect of the coexistence of Cu^{2+} ions on the adsorption of ACHF for Hg^{2+} was also investigated, and the experiment results (as provided in Table V) indicated that the residual concentration of Hg^{2+} reached zero after adsorption with the coexistence of Cu^{2+} ions in the concentration range 0–1000 mg/L. That is, the existence of Cu^{2+} ions did not affect the adsorption of ACHF for Hg^{2+}. It appeared that the fiber had a high selectivity for Hg^{2+} ions in the presence of Cu^{2+} at different initial concentrations.

CONCLUSIONS

A chelating fiber with amino groups (ACHF) was prepared by preirradiation grafting and consequent amination. Mechanical tests showed that ACHF had better elasticity and flexibility and possessed considerable thermal stability. The fiber ACHF had good adsorption for Hg^{2+}, and its maximum adsorption capacity for Hg^{2+} was up to 785 mg/g, which indicated a remarkable capacity compared to many other adsorbents. At the same time, the fiber had a high selectively for mercury, even when Cu^{2+} coexisted at different concentrations. The fiber could get rid of trace mercury in water to meet the allowable concentration of Hg^{2+} for drinking water. The fiber has great feasibility and potential for large-scale application in heavy-metal-ion wastewater treatment. The effect of other foreign ions, such as Ca^{2+} and Mg^{2+} that have high concentrations in drinking

TABLE IV
Kinetic Parameters and Correlation Coefficients of the Two Kinds of Kinetic Equations for the Adsorption Rate

	Pseudo-first-order equation			Pseudo-second-order equation		
C_0	Q_e	k_1	R^2	Q_e	k_2	R^2
500 μg/L	0.81 μg/g	0.105	0.790	0.82 μg/g	0.950	0.999
123 mg/L	91.87 mg/g	0.022	0.987	95.60 mg/g	4.53×10^{-4}	0.997

TABLE V
Amount of Hg^{2+} Adsorption on ACHF with Cu^{2+} Coexisting in the Solution

Concentration of Cu^{2+} (mg/L)	0	100	200	400	600	800	1000
Initial concentration of Hg^{2+} (mg/L)	100	100	100	100	100	100	100
Residual concentration of Hg^{2+} (mg/L)	0	0	0	0	0	0	0.08

water or groundwater and the reversibility of Hg^{2+} adsorption will be studied in the future.

References

1. Boening, D. W. Chemosphere 2000, 40, 1335.
2. Grandjean, P. International Encyclopedia of Public Health; Academic: San Diego, 2008; p 434.
3. Tchounwou, P. B.; Ayensu, W. K.; Ninashvili, N.; Sutton, D. Environ Toxicol Water Qual 2003, 18, 149.
4. Clarkson, T. W. J Trace Elem Exp Med 1998, 11, 303.
5. Natale, F. D.; Lancia, A.; Molino, A. J Hazard Mater 2006, 132, 220.
6. Hutchison, A. R.; Atwood, D. A. J Chem Crystallogr 2003, 33, 631.
7. Hollerman, W.; Holland, L.; Ila, D.; Hensley, J.; Southworth, G.; Klasson, T.; Taylor, P.; Johnston, J.; Turner, R.; Hollerman, W.; Holland, L.; Ila, D. J Hazard Mater 1999, 68, 193.
8. Monteagudo, J. M.; Ortiz, M. J. J Chem Technol Biotechnol 2000, 75, 767.
9. Chojnacki, A.; Chojnacka, K.; Hoffmann, J.; Górecki, H. Miner Eng 2004, 17, 933.
10. Gash, A. E.; Spain, A. L.; Dysleski, L. M.; Flaschenriem, C. J.; Kalaveshi, A.; Dorhout, P. K.; Strauss, S. H. Environ Sci Technol 1998, 32, 1007.
11. Yardim, M. F.; Budinova, T.; Ekinci, E.; Petrov, N.; Razvigorova, M.; Minkova, V. Chemosphere 2003, 52, 835.
12. Kadirvelu, K.; Kavipriya, M.; Karthika, C.; Vennilamani, N.; Pattabhi, S. Carbon 2004, 42, 745.
13. Pérez-Quintanilla, D.; Hierro, I. D.; Fajardo, M.; Sierra, I. J Hazard Mater 2006, 134, 245.
14. Dujardin, M. C.; Cazé, C.; Vroman, I. React Funct Polym 2000, 43, 123.
15. Liu, C. Q.; Huang, Y. Q.; Naismith, N.; Economy, J.; Talbott, J. Environ Sci Technol 2003, 37, 4261.
16. Wang, C. C.; Chen, C. Y.; Chang, C. Y. J Appl Polym Sci 2002, 84, 1353.
17. Rivas, B. L.; Jara, M.; Pereira, E. D. J Appl Polym Sci 2003, 89, 2852.
18. Beatty, S. T.; Fischer, R. J.; Hagers, D. L.; Rosenberg, E. Ind Eng Chem Res 1999, 38, 4402.
19. Kiefer, R.; Höll, W. H. Ind Eng Chem Res 2001, 40, 4570.
20. Zeng, H. M. Functional Fibers, 1st ed.; Chemical Industry Press: Beijing, 2005.
21. Docquir, F.; Toufar, H.; Su, B. L. Langmuir 2001, 17, 6282.
22. Choi, S. H.; Nho, Y. C.; Kim, G. T. J Appl Polym Sci 1999, 71, 643.
23. Choi, S. H.; Nho, Y. C. J Appl Polym Sci 1999, 71, 999.
24. Grasselli, M.; Cañizo, A. A.; Camperi, S. A.; Wolman, F. J.; Smolko, E. E.; Cascone, O. Radiat Phys Chem 1999, 55, 203.
25. Konishi, S.; Saito, K.; Furusaki, S.; Sugo, T. J Membr Sci 1996, 111, 1.